

Medium effects on the flow of strange particles in heavy ion collisions

Che Ming Ko^{†§}

[†] Cyclotron Institute and Physics Department, Texas A&M University, College Station, Texas 77843-3366, USA

Abstract. Strange particles such as the kaon and lambda are useful in probing the properties of dense matter formed in heavy ion collisions. We review in this talk the theoretical understandings of their properties in nuclear medium based on both the effective chiral Lagrangian and the phenomenological hadronic model. We further review the effects due to changes in their in-medium properties on their collective flow in heavy ion collisions.

1. Introduction

Strange particle production from heavy ion collisions offers the possibility to study the properties of the hot dense matter formed in these collisions. Because of its small interaction cross section with a nucleon, about 10 mb, Randrup and Ko [1] suggested that the kaon would be a good messenger of the dense matter where it was expected to be produced in heavy ion collisions. The first experiment was carried out by Schnetzer *et al.* [2] at the Bevalac at an energy of 2.1 GeV/nucleon. Although the kaon yield was consistent with the prediction of cascade calculations, the momentum spectra of kaons could only be explained if the final-state scattering of kaons was included [3, 4]. Subsequently, Aichelin and Ko [5] showed that the kaon yield in heavy ion collisions at subthreshold energies, i.e., below 1.56 GeV/nucleon, was sensitive to the nuclear equation of state used in the transport model. Comparisons of the experimental data from the KaoS collaboration at SIS/GSI [6] with results from various transport models seem to indicate that the nuclear equation of state is soft [7, 8, 9], consistent with that inferred from the proton flow data [10].

As to the antikaon, Kaplan and Nelson [11] pointed out, based on the chiral Lagrangian, that its mass should decrease in dense matter due to the attractive vector and scalar potentials, the latter resulting from the explicit chiral symmetry breaking, leading to a possible kaon condensation in neutron stars [12]. This would limit the maximum mass of neutron stars to about one and a half solar masses and give rise to suggestions of many small black holes in our galaxy [13]. The drop of antikaon mass also gives a natural explanation [14] of the observed enhancement of subthreshold antikaon production in heavy ion collisions by the FOPI collaboration at SIS/GSI [15].

Using the relativistic transport model [16], Li *et al.* [17] showed that the kaon directed flow in heavy ion collisions was sensitive to the strength of kaon potential in

[§] To whom correspondence should be addressed (ko@comp.tamu.edu)

nuclear medium. The observed vanishing kaon flow by the FOPI collaboration [18] was found to be consistent with the prediction based on the repulsive kaon potential that results from the cancellation of the attractive scalar and repulsive vector potentials acting on the kaon. Analyses of the the experimental data from heavy ion collisions at AGS/BNL and SPS/CERN are being carried out, and preliminary results cannot be explained without including the kaon medium effects in the transport model.

In this talk, we will review the theoretical understandings of the properties of kaon and lambda in nuclear medium, and the effects due to changes in their in-medium properties on their collective flow in heavy ion collisions at SIS/GSI, AGS/BNL, and SPS/CERN.

2. Strange particles in nuclear medium

2.1. Kaon and antikaon

Since the pioneering work of Kaplan and Nelson [11], there were many studies on the properties of kaons in dense matter using the chiral Lagrangian [19]. To leading order in the expansion of the chiral Lagrangian, the explicit symmetry breaking term gives rise to the large kaon mass, while the term involving the vector current contributes to its isoscalar s -wave scattering amplitude from a nucleon. The latter leads to a repulsive or an attractive optical potential for K^+ and K^- in symmetric nuclear matter. Further attraction for the kaon is obtained from terms next to leading order in the chiral expansion, which involves the kaon-nucleon sigma term and depends again on the explicit symmetry breaking. Ignoring isospin dependent terms, which do not contribute in symmetric nuclear matter, the chiral Lagrangian to the next to leading order is

$$\begin{aligned} \mathcal{L}_{KN} = & -\frac{3}{8f^2}\bar{N}\gamma_\mu N(\bar{K}\overset{\leftrightarrow}{\partial}^\mu K) + \frac{\Sigma_{KN}}{f^2}\bar{N}N\bar{K}K \\ & + \frac{\tilde{D}}{f^2}(\bar{N}N)(\partial_\mu\bar{K}\partial^\mu K). \end{aligned} \quad (1)$$

In the above, $f \sim 93$ MeV is the pion decay constant, and the value of the kaon-nucleon sigma-term $\Sigma_{KN} = \frac{1}{2}(m_q + m_s)\langle N|\bar{u}u + \bar{s}s|N\rangle$ depends on the strangeness content of the nucleon, $y = 2\langle N|\bar{s}s|N\rangle/\langle N|\bar{u}u + \bar{d}d|N\rangle \sim 0.1 - 0.2$. Using the light quark mass ratio $m_s/m_{u,d} \sim 29$, one obtains $370 < \Sigma_{KN} < 405$ MeV. On the other hand, lattice gauge calculations show that $y \sim 0.33$ which would give $\Sigma_{KN} \sim 450$ MeV [20]. The additional parameter, $\tilde{D} \approx 0.33/m_K - \Sigma_{KN}/m_K^2$, is determined from comparing with K^+ -nucleon scattering data.

In the mean-field approximation, the kaon energy in the nuclear medium is then given by

$$\begin{aligned} \omega_{K,\bar{K}} = & \left[\sqrt{(m_K^{*2} + k^2) \left(1 + \frac{\tilde{D}}{f^2}\rho_s\right)^2 + \left(\frac{3}{8f^2}\rho_N\right)^2} \pm \frac{3}{8f^2}\rho_N \right] \\ & \times \left(1 + \frac{\tilde{D}}{f^2}\rho_s\right)^{-1}, \end{aligned} \quad (2)$$

with

$$m_K^* = \sqrt{\left(m_K^2 - \frac{\Sigma_{KN}}{f^2}\rho_s\right)\left(1 + \frac{\tilde{D}}{f^2}\rho_s\right)^{-1}}. \quad (3)$$

In the above, the plus and minus signs are for the kaon and antikaon, respectively. Using the KFSR relation ($m_\rho = 2\sqrt{2}fg_\rho$) and the SU(3) relation ($g_\omega = 3g_\rho$), the kaon vector potential, $3\rho_N/(8f^2)$, can be written as $(1/3)(g_\omega/m_\omega)^2\rho_N$ which is just 1/3 of the nucleon vector potential in the Walecka model [21], as expected from the constituent quark model. With $\Sigma_{KN} \sim 350$ MeV, the in-medium kaon mass at normal nuclear matter density, given by its energy at zero three-momentum, increases by about 30 MeV, consistent with that given by the impulse approximation using the kaon-nucleon scattering length, while that of antikaon decreases by about 100 MeV, similar to that extracted from the kaonic atom data [22]. The kaon and antikaon potential from the chiral Lagrangian are shown in the left panel of Fig. 1 by the dotted and dashed curves for Σ_{KN} equal to 270 and 450 MeV, respectively.

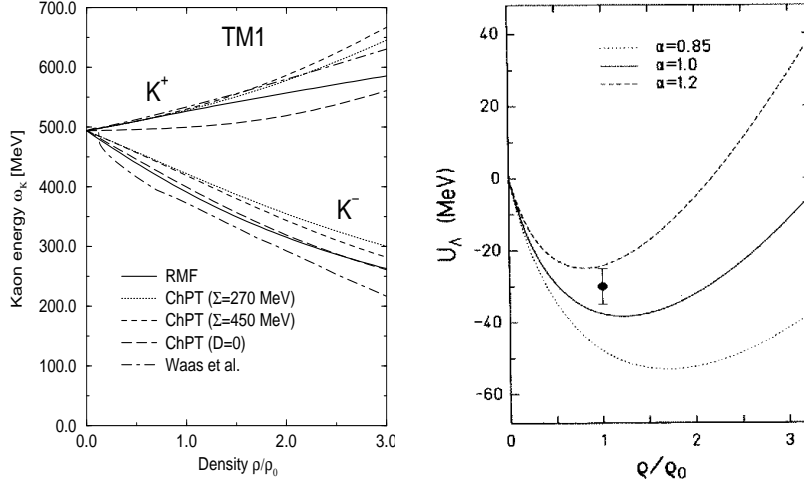


Figure 1. Left panel: Kaon and antikaon potential. Right panel: Lambda potential for different values of repulsive vector potential. The empirical value from the hypernuclear properties is shown by the filled circle.

The chiral Lagrangian predicts, however, an attractive isoscalar s-wave scattering length for the K^- -nucleon scattering amplitude, which contradicts with the repulsive one found in experiments [23]. This discrepancy has been attributed to the existence of the $\Lambda(1405)$ which is located below the K^-N -threshold. To circumvent this problem, the chiral perturbation calculation was extended either by Lee *et al.* [24] to include an explicit $\Lambda(1405)$ state or by Kaiser *et al.* [25] to use the interaction obtained from the leading order chiral Lagrangian as a kernel for a Lippman-Schwinger type calculation, which was then solved to generate a bound state $\Lambda(1405)$. In this picture, the properties of the $\Lambda(1405)$ is significantly changed in the nuclear medium as a result of the Pauli blocking of the proton inside this bound state [26]. With increasing density, its mass increases and the strength of the resonance is reduced, leading to a change of the K^- optical potential from repulsive to attractive at a density of about

1/4 of nuclear matter density in agreement with the analysis of K^- atoms [22]. The resulting antikaon potential [27] is shown in the left panel of Fig. 1 by the dash-dotted curve.

The kaon potential was also studied in the meson-exchange model by Schaffner *et al.* [28] based on the Lagrangian

$$\mathcal{L} = \partial_\mu \bar{K} \partial^\mu K - (m_K^2 - g_{\sigma K} m_K \sigma) \bar{K} K + i g_{\omega K} \omega_\mu \bar{K} \overleftrightarrow{\partial}^\mu K, \quad (4)$$

where the coupling constants $g_{\sigma K}$ and $g_{\omega K}$ to the scalar (σ) and vector (ω) fields, respectively, can be related to other known coupling constants using SU(3) symmetry or determined empirically from the kaon-nucleon scattering amplitude. In the mean-field approximation, the kaon energy is then given by

$$\omega_{K,\bar{K}} = [m_K^2 + k^2 - g_{\sigma K} m_K \sigma + (g_{\omega K} \omega_0)^2]^{1/2} \pm g_{\omega K} \omega_0, \quad (5)$$

where the plus and minus signs are, again, for the kaon and antikaon, respectively. The kaon potential given by this model is shown in the left panel of Fig. 1 by the solid curve. Although all theoretical models predict that the kaon has a moderate repulsive potential and the antikaon has a strong attractive potential, their magnitudes differ substantially. It is thus important to have experimental data to constrain the values of the kaon and antikaon potentials. Kaon production from heavy ion collisions offers this possibility, particularly for the kaon potential at high densities.

For the momentum dependence of kaon potential, Shuryak [29] found, based on the impulse approximation, that it would become weaker as its momentum increases. On the other hand, the dispersion relation analysis by Sibirtsev and Cassing [30] shows that the kaon potential is essentially independent of the momentum. They also found that the antikaon potential became less attractive with increasing momentum. In a coupled channel approach involving $\bar{K}N$, $\pi\Sigma$, and $\Lambda(1405)$, Schaffner-Bielich *et al.* [31] found that the antikaon potential could even change to a repulsive one at large momenta due to the diminishing effect of the Pauli blocking. The latter effect was shown to be further enhanced in nuclear matter at finite temperature.

2.2. Lambda

Because of strangeness conservation, hyperons such as the lambda and sigma are produced together with kaons. Heavy ion collisions thus also offer the opportunity to study the properties of hyperons in dense matter, which is important in understanding if the core of a neutron star can exist as a hyperon matter [32]. The potential for the lambda particle at normal nuclear matter density is relatively well determined to be about -30 MeV from the structure of hypernuclei [33]. Theoretically, the lambda potential in nuclear matter has been studied using the Dirac-Bruckner-Hartree-Fock approach [34]. The result ranges from -25 to -40 MeV, depending on the input boson-exchange models for the ΛN interaction. There were also various attempts to generalize the Walecka-type model from SU(2) to SU(3) to include the hyperon degrees of freedom [35]. In the naive SU(3) quark model, the hyperon potential is about 2/3 of the nucleon potential, as there are only two light quarks in a hyperon instead of three light quarks in a nucleon. Recently, hyperon properties in nuclear matter were also studied using the QCD sum-rule approach. It was found that both lambda scalar and vector potentials were significantly weaker than the prediction from the naive quark model [36], while those of the sigma hyperon were somewhat stronger and were close to the ones for the nucleon [37]. The accuracy of these findings were,

however, limited by uncertainties in the nucleon strangeness content and certain in-medium four-quark condensates.

Writing the lambda self-energy in terms of the scalar (Σ_S^Λ) and vector (Σ_V^Λ) parts, its potential can then be expressed as

$$U_\Lambda(\mathbf{p}, \rho) = [(m_\Lambda - \Sigma_S^\Lambda)^2 + \mathbf{p}^2]^{1/2} + \Sigma_V^\Lambda - (m_\Lambda^2 + \mathbf{p}^2)^{1/2}. \quad (6)$$

Using $\Sigma_S^\Lambda \sim 2\Sigma_S^N/3$ and $\Sigma_V^\Lambda \sim 2\alpha\Sigma_V^N/3$, where Σ_S^N and Σ_V^N are the nucleon scalar and vector self-energies, respectively, the lambda potential is shown in the right panel of Fig. 1 for different values of α . Also shown in the figure is the empirical lambda potential at normal nuclear matter density.

3. Strange particle flow in heavy ion collisions

Strange particle flow in heavy ion collisions is sensitive to the mean-field potential in dense matter as an attractive interaction between the strange particle and nucleons aligns its flow with that of the nucleons whereas a repulsion leads to an anti-alignment (anti-flow). However, strange particle flow is also sensitive to the overall reaction dynamics, in particular to the properties of the nuclear mean field and to reabsorption processes especially in case of the antikaons. Therefore, transport calculations are required in order to consistently incorporate all these effects.

3.1. GSI

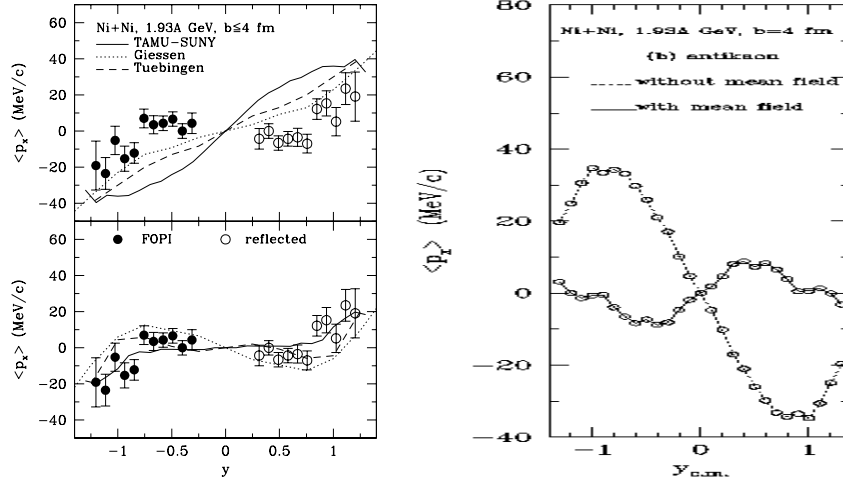


Figure 2. Kaon (left panel) and antikaon (right panel) flow.

The K^+ flow has been measured by the FOPI collaboration [18] at GSI. Although the error bars are large, the data (circles) in the left panel of Fig. 2 clearly show a vanishing flow at midrapidity. Also shown in the figure are theoretical results from the transport model calculations by the TAMU-SUNY group [17, 38], the Giessen group [39], and the Tübingen group [40]. It is seen that the experimental data are consistent with the results that include the kaon mean-field potential from the chiral Lagrangian (lower left panel) but not the ones without any potential (upper left panel). It is worthwhile to point out that while the primordial flow of kaons produced from

meson-baryon scattering is positive, those produced from baryon-baryon collisions already have a very small flow [41]. Also, it has been found that inclusion of the spatial component of the kaon vector potential would lead to an attractive Lorentz force between the kaon and nucleons, leading thus again to a positive kaon flow [42]. However, the Lorentz force increases with kaon momentum, and this contradicts the predictions from more detailed theoretical studies which show an opposite momentum dependence [29, 30].

The repulsive kaon potential also leads to an enhanced emission of kaons out of the reaction plane as first shown by Li and Ko [43]. Similar results, shown in the left panel of Fig. 3, were obtained by the Tübingen group [44]. The observed kaon azimuthal distribution, which shows an enhanced out-of-plane emission, can only be explained by the inclusion of a repulsive kaon potential. Again, the data do not support the existence of a simple Lorentz force between the kaon and nucleons.

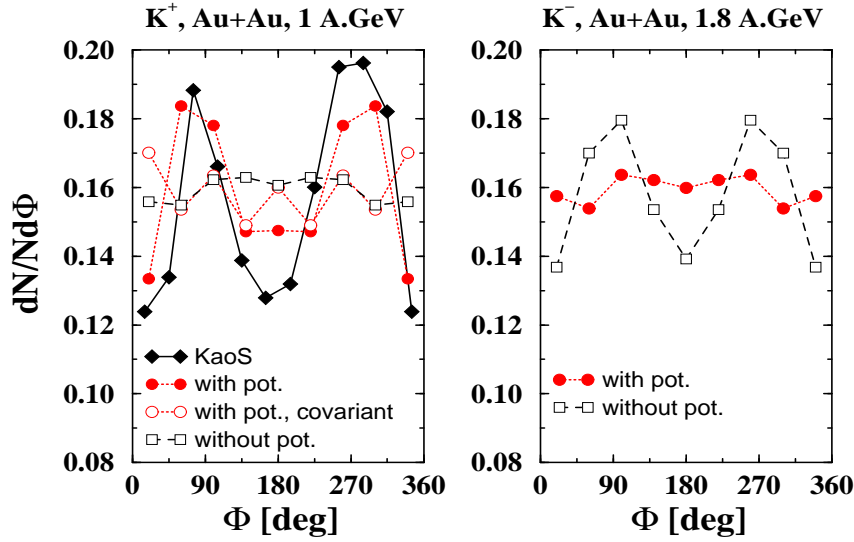


Figure 3. Azimuthal distributions of K^+ (left panel) and K^- (right panel) from Ref. [44].

For antikaons, Li and Ko [45] showed that their flow and azimuthal distribution were influenced by the attractive potential. In the right panel of Fig. 3, the results from the Tübingen group [44] show that the K^- azimuthal distribution, which is dominated by out-of-plane emission in the absence of potential, becomes more symmetric once the attractive potential is included in the relativistic transport model. Similarly, the antiflow of antikaons in the absence of potential, which results from the strong absorption effect, changes into a positive flow under the influence of the attractive potential. The results from Li and Ko are shown in the right panel of Fig. 2. Unfortunately, the measurement of K^- observables is more difficult since it is produced less abundantly at subthreshold energies.

For lambda particles, which cannot be absorbed as the pion and antikaon, it is expected to have a positive flow as the nucleons. Li and Ko [46] found that the magnitude of the lambda flow depended on the strength of the attractive lambda potential. In the left panel of Fig. 4, theoretical results from Li and Brown [38] are shown together with the experimental data from the FOPI collaboration [18]. Both

the lambda-nucleon scattering and the attractive potential are seen to increase the flow. However, the large experimental errors in the data makes it not possible to draw conclusions on the magnitude of the lambda potential. A similar conclusion was reached by the Tübingen group [47]. Also shown in the right panel of Fig. 4 is the lambda azimuthal distribution predicted by Li and Ko [46]. It is seen that the lambda potential has a large effect on the lambda azimuthal distribution. It will be of interest to compare the theoretical predictions with future experimental data.

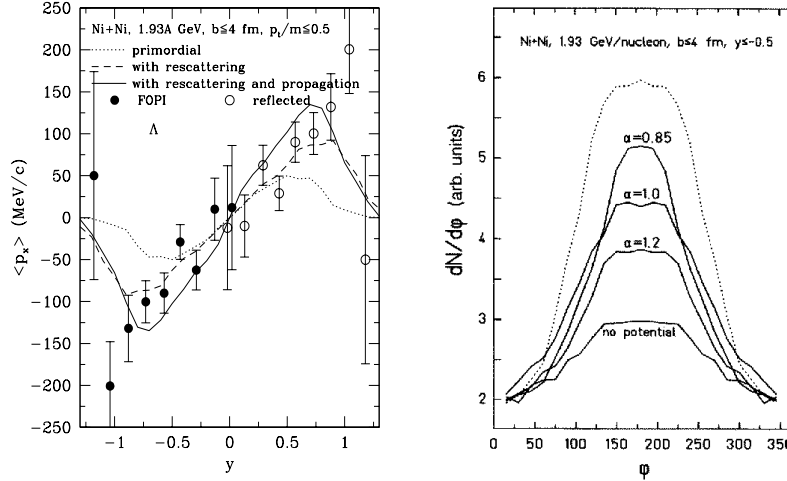


Figure 4. Lambda flow (left panel) and azimuthal distribution (right panel).

3.2. AGS

Both lambda and kaon flow were measured in Au+Au collisions at 6 A GeV at AGS by the E895 Collaboration [48, 49]. The data show a positive lambda flow and a large kaon antflow. To understand these results, Zhang *et al.* [50] and Pal *et al.* [51] have carried out a calculation based on the ART transport model [52]. In the left panel of Fig. 5, the theoretical results from Ref. [50] are compared with the measured lambda (filled circles) and proton (squares) flow. The proton flow is well described by a soft nuclear equation of state corresponding to an incompressibility of 200 MeV (solid curve). The results from a stiff equation of state with $K = 380$ MeV is seen to give too large a proton flow. This is different from the conclusion based on the UrQMD model [53], which includes the string dynamics in the initial stage, that the stiff equation of state describes the data better. Although the lambda flow obtained with a potential gives a good description of the data, the large experimental errors cannot differentiate the difference between a lambda potential which is 2/3 of the nucleon potential (dotted curve) and that which is the same as the nucleon one (dot-dashed curve). Also shown is the result obtained with a lambda potential which is 2/3 of the nucleon potential but without the lambda-nucleon scattering (dashed curve). Comparing it with the dotted curve shows that the scattering effect is not large.

For the kaon flow, the experimental data (circles) show a very large antflow

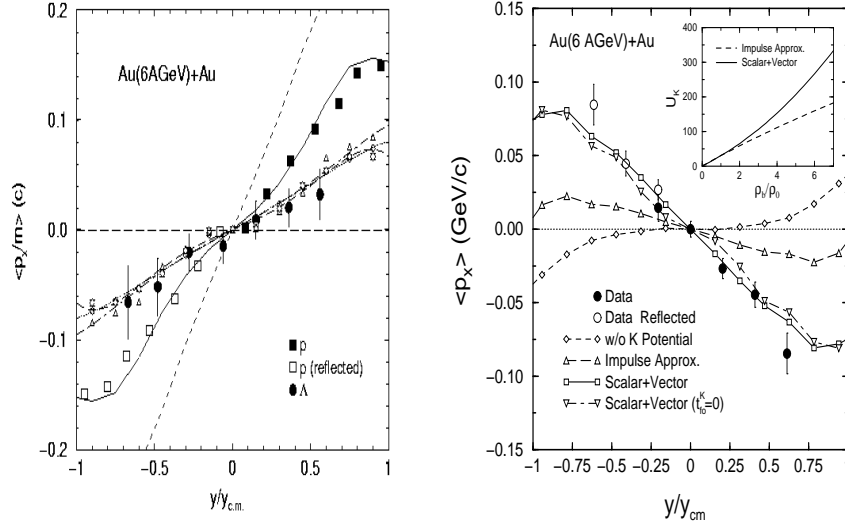


Figure 5. Proton and lambda (left panel) as well as kaon (right panel) directed flow.

compared to that in heavy ion collisions at lower energies available from GSI. This is shown in the right panel of Fig. 5 together with the theoretical results obtained from the ART model using various kaon potentials [51]. Without potential (dashed curve), the kaon has a positive flow, which is similar to the results obtained from the RQMD model [49]. With the potential obtained from the impulse approximation, shown by the dashed curve in the inset, the kaon flow (dashed curve) changes to a small negative one. The results (solid curve) obtained from the kaon potential given by the chiral Lagrangian, shown by the solid curve in the inset, agree very well with the large kaon antflow measured in experiments. The latter potential is seen to be more repulsive at high densities than the one given by the impulse approximation. This is due to the saturation of the scalar density with increasing densities, which makes the attractive scalar kaon potential less important at high densities than the repulsive vector kaon potential, which increases with density. Setting the kaon formation time to zero ($t_{fo}^K = 0$) (dash-dotted curve) does not affect much the result. Li *et al.* [54] have pointed out that the kaon flow is better illustrated by its dependence on the transverse momentum, i.e., the differential flow. The decrease of kaon flow is then due to the cancellation between the negative flow of kaons with low transverse momenta and the positive flow of kaons with high momenta.

The K^- flow was also studied in the ART model by Song *et al.* [55] for heavy ion collisions at AGS energies. Similar to the results at GSI energies, the K^- was predicted to have a positive flow due to the strong attractive potential. However, there are at present no experimental data from AGS on the antikaon flow.

3.3. SPS

For heavy ion collisions at SPS energies, there is very little study on the flow of strange particles. Experiments by the WA98 collaboration [56] show that the kaon elliptic flow, which measures the asymmetry between the in-plane and out-of-plane kaon momentum

distributions, is negative, opposite to that for the proton and the pion. This implies that kaons are preferentially emitted out of the reaction plane. Theoretical results from the RQMD without the kaon potential show instead a positive kaon elliptic flow. Whether the observed negative kaon elliptic flow is due to the repulsive kaon potential remains to be studied.

4. Summary

We have reviewed in this talk the kaon in-medium properties based on the chiral Lagrangian, which predicts that the kaon feels a moderate repulsive potential due to the cancellation of the attractive scalar and repulsive vector potentials while the antikaon has a strong attractive potential as the vector repulsion becomes attractive for the antikaon. These results are consistent with the empirical information obtained from the K^+ -nucleus scattering and the kaonic atom. Similar results are obtained from the phenomenological meson-exchange model. The latter model also allows one to study the lambda potential, which is predicted to have a potential which is somewhat less attractive than that for a nucleon.

We have also reviewed the experimental data for both kaon and lambda flow in heavy ion collisions at various energies. For the GSI energies, both the vanishing kaon flow and enhanced out-of-plane emission are consistent with the repulsive potential predicted by the chiral Lagrangian. The predicted positive flow of antikaons and their more symmetric azimuthal distribution remain to be verified by experiments. For the lambda flow, which is positive in the experiments, the data are not accurate enough to allow for a determination of the strength of the lambda potential. However, the effect of potential is predicted to be large in the lambda azimuthal distribution.

For heavy ion collisions at AGS, the large antiflow of kaons observed in the experiments is again consistent with the kaon potential predicted by the chiral Lagrangian, which shows that it becomes more repulsive at high densities than that given by the impulse approximation based on the kaon-nucleon scattering length. Again, the lambda potential cannot be determined from the lambda flow data due to the large errors in the experiment. Also, there is no data to compare with the theoretically predicted positive flow of antikaons.

For heavy ion collisions at SPS, there are very little experimental measurements on the flow of strange particles. Preliminary results of a negative kaon elliptic flow, i.e. out-of-plane emission dominates over in-plane flow, cannot be accounted for by transport model studies without a kaon mean-field potential. Further theoretical and experimental studies are thus needed in order to understand the properties of strange particles in the hot dense matter formed in such high energy heavy ion collisions.

5. Acknowledgments

This work is supported by the National Science Foundation under Grant No. PHY-9870038, the Welch Foundation under Grant No. A-1358, and the Texas Advanced Research Program under Grant No. FY99-010366-0081.

6. References

- [1] Randrup J and Ko C M 1980 *Nucl. Phys. A* **343** 519; 1983 *ibid.* **411** 537
- [2] Schnetzer S *et al* 1982 *Phys. Rev. Lett.* **49** 989

- [3] Randrup J 1981 *Phys. Lett.* **99B** 9
- [4] Ko C M 1981 *Phys. Rev. C* **23** 2760
- [5] Aichelin J and Ko C M 1985 *Phys. Rev. Lett.* **55** 2661
- [6] Miskowiec D *et al* 1994 *Phys. Rev. Lett.* **72** 3650
- [7] Li G Q and Ko C M 1995 *Phys. Lett.* **349B** 405
- [8] Maruyama T, Cassing W, Mosel U, Teis S and Weber K 1994 *Nucl. Phys. A* **573** 536
- [9] Hartnack C, Jaenicke J and Aichelin J 1994 *Nucl. Phys. A* **580** 643
- [10] Pan Q B and Danielewicz P 1993 *Phys. Rev. Lett.* **70** 2062; Zhang J, Das Gupta S and Gale C 1994 *Phys. Rev. C* **50** 1617.
- [11] Kaplan D B and Nelson A E 1986 *Phys. Lett.* **175B** 57; 1987 *ibid.* **192B** 193
- [12] Brown G E, Kubodera K, Page D and Pizzocherri P 1988 *Phys. Rev. D* **37** 2042
- [13] Brown G E and Bethe H A 1994 *Astrophys. J.* **423** 659
- [14] Li G Q, Ko C M and Fang X S 1994 *Phys. Lett.* **329B** 149
- [15] Schröter A *et al* 1994 *Z. Phys. A* **350** 101
- [16] Ko C M, Li Q and R Wang 1987 *Phys. Rev. Lett.* **59** 1084; Ko C M and Li Q 1988 *Phys. Rev. C* **37** 2270; Li Q, Wu J Q and Ko C M 1989 *Phys. Rev. C* **39** 849
- [17] Li G Q, Ko C M and Li B A, 1995 *Phys. Rev. Lett.* **74** 235; Li G Q and Ko C M 1995 *Nucl. Phys. A* **594** 460
- [18] Ritman J 1995 *Z. Phys. A* **352** 355
- [19] Brown G E, Kubodera K and Rho M 1987 *Phys. Lett.* **192B** 273; Lynn B W, Nelson A E and Tetrads N 1990 *Nucl. Phys. B* **345** 186; Politzer H D and Wise M B 1991 *Phys. Lett.* **273B** 156; Muto T and Tatsumi T 1992 *Phys. Lett.* **283B** 165; Brown G E, Ko C M and Kubodera K 1992 *Z. Phys. A* **341** 301; Yabu H *et al* 1993 *Phys. Lett.* **315B** 17; Lutz M, Steiner A and Weise W 1994 *Nucl. Phys. A* **574** 755; Lee C H *et al* 1995 *Nucl. Phys. A* **585** 401.
- [20] Dong S J and Liu K F 1995 *Nucl. Phys. B* **42** 322; Fukugita M *et al* 1995 *Phys. Rev. D* **51** 5319
- [21] Serot B. D and Walecka J D 1986 *Adv. Nucl. Phys.* **16** 1
- [22] Friedman E, Gal A and Batty C J 1993 *Phys. Lett.* **308B** 6; 1994 *Nucl. Phys. A* **579** 518
- [23] Martin A D 1981 *Nucl. Phys. A* **179** 33
- [24] Lee C H, Brown G E and Rho M 1994 *Phys. Lett.* **335B** 266
- [25] Kaiser N, Siegel P B and Weise W 1995 *Nucl. Phys. A* **594** 325
- [26] Koch V 1994 *Phys. Lett.* **337B** 7
- [27] Waas T, Kaiser N and Weise W 1996 *Phys. Lett.* **36B** 12
- [28] Schaffner J, Bondorf J and Mishustin I N 1997 *Nucl. Phys. A* **625** 325
- [29] Shuryak E and Thorsson V 1992 *Nucl. Phys. A* **536** 739
- [30] Sibirtsev A and Cassing W 1998 *Nucl. Phys. A* **641** 476
- [31] Schaffner-Bielich J, Koch V and Effenberger M 2000 *Nucl. Phys. A* **669** 153
- [32] Glendenning N K 1991 *Phys. Rev. Lett.* **67** 2424
- [33] Gibson B F and Hungerford III E V 1995 *Phys. Rep.* **257** 349
- [34] Reuber A, Holinde K and Speth J 1994 *Nucl. Phys. A* **570** 543
- [35] Brockmann R and Weise W 1977 *Phys. Lett.* **69B** 167; Boussy A 1977 *Nucl. Phys. A* **290** 324
- [36] Jin X and Nielsen 1995 *Phys. Rev. C* **51** 347
- [37] Jin X and Furnstahl R J 1994 *Phys. Rev. C* **49** 1190
- [38] Li G Q and Brown G E 1998 *Nucl. Phys. A* **636** 4887
- [39] Bratkovskaya E L, Cassing W and Mosel U 1997 *Nucl. Phys. A* **622** 593
- [40] Wang Z S *et al* 1998 *Nucl. Phys. A* **628** 151
- [41] David C, Hartnack C and Aichelin J 1999 *Nucl. Phys. A* **650** 358
- [42] Fuchs C, Kosov D S, Faessler A, Wang Z S and Waindzoeh T 1998 *Phys. Rev. C* **57** 3284
- [43] Li G Q and Ko C M 1996 *Phys. Lett.* **381B** 17
- [44] Wang Z S, Fuchs C, Faessler A and Bross-Boelting T 1999 *Euro. Phys. Jour. A* **5** 275
- [45] Li G Q and Ko C M 1996 *Phys. Rev. C* **54** R2159
- [46] Li G Q and Ko C M 1996 *Phys. Rev. C* **54** 1897
- [47] Wang Z S, Faessler A, Fuchs C and Waindzoeh T 1998 *nucl-th/9811090*
- [48] Liu H *et al* 2000 *Phys. Rev. Lett.* in press
- [49] Chung P *et al* 2000 *Phys. Rev. Lett.* in press
- [50] Zhang B, Ko C M, Li B A and sustich A T 2000 *J. Phys. G* in press; *nucl-th/9906067*.
- [51] Pal S, Ko C M, Lin Z and Zhang B 2000 *Phys. Rev. C* submitted
- [52] Li B A and Ko C M 1995 *Phys. Rev. C* **52** 2037
- [53] Soff S, Bass A, Bleicher M, Stöcker H and Greiner G *nucl-th/9903061*.
- [54] Li B A, B Zhang, Sustich A T and Ko C M 1999 *Phys. Rev. C* **60** 034902
- [55] Song G, Li B A and Ko C M 1999 *Nucl. Phys. A* **646** 481
- [56] Aggarwal M M *et al* 1998 *Phys. Lett.* **420B** 169